Anisotropic Median Filtering for Stereo Disparity Map Refinement

Nils Einecke and Julian Eggert
Honda Research Institute Europe GmbH, Carl-Legien-Strasse 30, 63073 Offenbach/Main, Germany

Keywords: Stereo Vision, Refinement, Anisotropic Filter.

Abstract: In this paper we present a novel method for refining stereo disparity maps that is inspired by both simple median filtering and edge-preserving anisotropic filtering. We argue that a combination of these two techniques is particularly effective for reducing the fattening effect that typically occurs for block-matching stereo algorithms. Experiments show that the newly proposed post-refinement can propel simple patch-based algorithms to much higher ranks in the Middlebury stereo benchmark. Furthermore, a comparison to state-of-the-art methods for disparity refinement shows a similar accuracy improvement but at only a fraction of the computational effort. Hence, this approach can be used in systems with restricted computational power.

SCITEPRESS SCIENCE AND TECHNOLOGY PUBLICATIONS

1 INTRODUCTION

Despite many years of research stereoscopic depth estimation is still one of the most active fields in computer vision. However, the research is often governed by the goal to find ever more accurate algorithms without taking much regard to computational efficiency or algorithmic complexity. Because of this trend the developed methods are often not applicable in mobile[1] systems due to the restrictions in hardware and energy consumption such systems imply.

The main steps of a stereo algorithm (Scharstein and Szeliski, 2002) are *matching cost computation*, *matching cost aggregation*, *disparity calculation* and *disparity refinement*. Today, mobile robotic systems typically use block-matching with *summed absolute difference* (SAD), *normalized cross-correlation* (NCC) or *census* for the *cost computation* and extract the disparities by means of a simple winner-takes-all (WTA) mechanism. The *cost aggregation* step is either skipped or part of the actual cost like SAD while the *disparity refinement* usually reduces to a left-right consistency check, sometimes paired with a simple sub-pixel disparity interpolation. In contrast, high ranked algorithms are characterized by sophisticated *cost aggregation* and *disparity refinement* techniques that have runtimes of several seconds and often need to store and work on the full cost volume which is inappropriate for mobile systems.

In this paper, we take steps towards disparity map refinements whose memory and space complexity is comparable to block-matching stereo so that it can be used in combination. One prominent disadvantage of block-matching is the so called ”fattening effect” which describes the tendency of block-matching to lead to a spatial smoothing of disparity values. In particular, the fattening effect causes an imprecise location of depth discontinuities. The idea of the post-processing we present here is to reduce the fattening effect by employing an *anisotropic median* filtering. In contrast to a typical median filter, the proposed filter takes the local photometric structure of the scene into account.

[1]Here mobile system refers mainly to autonomous robotic systems.

2 RELATED WORK

According to (Scharstein and Szeliski, 2002) disparity map refinement is the last major step of a stereoscopic depth estimation and comes in several flavors. On the one hand, there are means for detecting and removing outliers. Arguably, the most often used technique is a left-right consistency check as for example introduced in (Fua, 1993). By calculating a stereo map for the left as well as for the right stereo image, inconsistencies in the disparity values are detected and removed. Furthermore, for local stereo algorithms it has been proposed in (Fua, 1993) to segment a disparity into regions of constant disparity and then to remove small regions as these are likely to be outliers.

Another typical refinement is to increase the resolution of the disparities by sub-pixel refinement. This can for example be done by fitting a curve to the matching cost (Fua, 1993; Matthies et al., 1989) or by iterative gradient descent techniques (Lucas and Kanade, 1981; Tian and Huhns, 1986). In general these methods allow for an increase of the depth resolution with little extra computational cost. In (Yang et al., 2007) Yang *et al*. present an iterative refinement for low-resolution depth images. They show that by using a bilateral filtering and sub-pixel interpolation one can achieve a reliable up-scaling of the disparity maps of up to three scales.

Besides the refinement techniques mentioned above, there are methods for improving disparity maps by imposing additional consistency constraints to the disparity or depth maps. For example Sun *et al*. (Sun et al., 2011) refine disparity maps by propagating disparity values along line segments. These segments are constructed such that they contain pixels of similar color. Within the segments reliable seed pixels are extracted whose disparity values are then propagated within the line segment. As the line segments contain pixels of similar color, the propagation enforces a smoothness constraint on the resulting map. In order to prevent streaking artifacts the refinement is completed with a voting scheme in vertical line segments and a bilateral filtering with a small filter size.

One drawback of the seed pixel propagation is that a lot of valuable information is thrown away since only the disparity values of the seed pixels are used to calculate the refined map. A different way is to enforce the smoothness by means of anisotropic image processing. The basic idea is to improve a pixel's disparity by considering all neighboring pixels weighted with their similarity. One way to achieve this is to apply anisotropic diffusion (Perona and Malik, 1990) to the disparity maps. Banno and Ikeuchi (Banno and Ikeuchi, 2009) showed that good results can be achieved by setting the diffusion coefficients dependent on color similarity and label confidence.

One interesting variant of anisotropic post-processing is the *local consistent* LC stereo method (Mattoccia, 2009). In LC the mutual relationship of neighboring pixels is modeled explicitly. This is done in a probabilistic fashion via pixel based functions that measure color and spatial proximity. Given these measures all disparity hypotheses of a point pair are evaluated for plausibility. The final disparity of a pixel is computed by accumulating the plausibilities within the corresponding image patch. Since the accumulated plausibilities depend on absolute and relative positions the LC approach constitutes also a sort of anisotropic processing. However, in contrast to the anisotropic diffusion there is no iterative processing, which makes this approach much faster.

It is important to note here, that anisotropic processing is not only restricted to the post-processing of disparity maps. A similar idea is also frequently used for cost aggregation by means of adaptively weighted filters (Yoon and Kweon, 2006; Heo et al., 2008). However, as such filters are non-separable they lead to a high computational costs. Even fast approximations need several seconds for standard disparity computations which prevents a reasonable application in mobile systems so far. Although anisotropic filters used for post-processing share the same problem of non-separability they have a runtime that is independent of the disparity search range because they are applied to the final disparity map.

Another advantage of working directly on the disparity maps is that this does not require information from the cost volume which dramatically reduces the memory footprint. This is in contrast to techniques of the *disparity optimization* step that precedes the *disparity refinement* step. Prominent examples for disparity optimization are dynamic programming (Scharstein and Szeliski, 2002; Wang et al., 2006) or scanline optimization (Scharstein and Szeliski, 2002; Hirschmüller, 2005). These techniques require at least some part of the cost volume at one time. Due to this, these methods are less suited for the restricted hardware in mobile systems. Here the anisotropic post-processing in conjunction with a local method in the disparity optimization step is more favorable.

An approach similar in spirit compared to our anisotropic median idea is the incorporation of an approximation of a local median filter into the energy minimization of optical flow methods (Sun et al., 2010). By using the relationship between median and L1 norm the energy minimization can be extended by an additional penalty term that implicitly enforces the effect of a subsequent median filter. In order to prevent the suppression of fine structures the L1 norm is weighted in accordance to the pixel similarity. Unfortunately, this approach is tailored for minimizing an energy function and, thus, incompatible with the fast block-matching methods with WTA characteristic that we target here.

3 ANISOTROPIC MEDIAN FILTERING

The main drawback of current anisotropic post-processing techniques is that they are still too computationally expensive for mobile systems. It has been shown (Mattoccia, 2010) for LC, that a more coarse grained processing leads to a substantial speed-

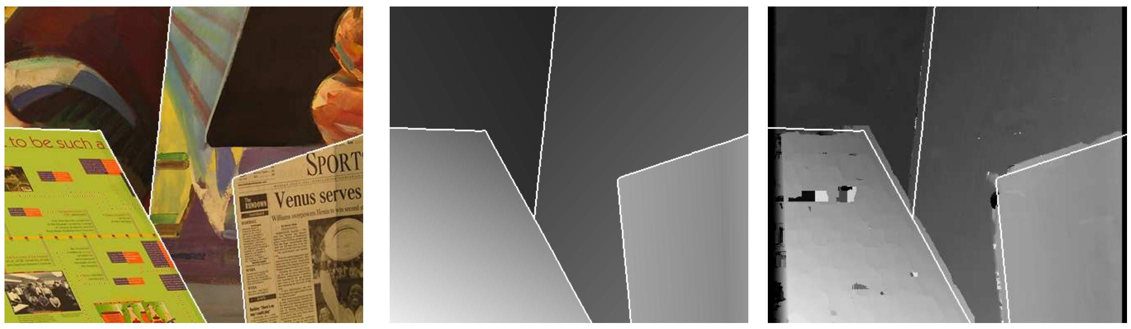

(a) Venus (b) Ground Truth (c) NCC Stereo

Figure 1: Visualization of the foreground fattening effect of block-matching stereo. (a) Venus image of the Middlebury benchmark and (b) the corresponding ground truth disparity map. (c) Disparity map calculated by means of block-matching stereo with NCC measure. The white lines in all three images visualize the discontinuities of the ground truth disparity. As can be seen in (c) the foreground disparities are smeared over background disparities.

SCITEPRESS SCIENCE AND TECHNOLOGY PUBLICATIONS

up, bringing the computational time on a standalone PC down to a few seconds while having only little or no degradation in accuracy. However, compared to the few hundreds of milliseconds it takes to compute a disparity map with a block-matching stereo method the anisotropic post-processing would govern the overall computational cost.

As has been discussed above, one major issue of block-matching stereo is the fattening effect at depth discontinuities which in most cases is a foreground fattening, i.e. foreground disparities suppress background disparities. To tackle this problem, we propose an anisotropic technique called *anisotropic median filtering* that is specifically tailored for reducing the fattening effect. Since median filtering is based on the well analyzed select problem, efficient algorithms for computing the median already exist. These algorithms can also be used for the anisotropic median for a fast processing.

Before coming to the algorithmic details let's have a look at a typical foreground fattening in Fig 1. This figure shows the Venus scene from the Middlebury benchmark (Scharstein and Szeliski, 2002) together with the ground truth disparity map and a disparity map computed by block-matching stereo with NCC. The ground truth disparity discontinuities are visualized via white lines. It can be observed in the block-matching disparity map that foreground disparities are strongly smeared over background disparities leading to a displacement of the disparity discontinuities.

Here our basic idea is to find a way to replace disparities that are inconsistent within their neighborhood with a new value that is in accordance to the neighboring values. There are two problems that arise. First, how to define neighborhoods and, second, how to extract a better disparity value from it. For the latter problem a median filter seems to be a good choice because it replaces statistical outliers with robust values. In disparity map refinement steps, median filters are typically used to remove peak-like outliers by considering a small rectangular neighborhoods around each pixel. Let $N(f)$ be the set of neighborhood pixels of a pixel f. Then the disparity $d(f)$ of f is replaced by

$$d(f) = \phi(D(f), \lceil \frac{n}{2} \rceil)\,, \tag{1}$$

where $D(f)$ is the list of all disparities in $N(f)$, $n = |N(f)|$ and $\phi(L,k)$ returns the k-th largest element of list L. Please note that we do not use the statistical definition of the median which would involve an averaging of two values in case of an even number of elements. Instead, we use the typical convention in image processing and computational theory that the median is always the lower median.

Although this reliably removes outliers it leaves fattened areas mainly untouched. The reason is that the neighborhood of a pixel near a depth discontinuity is likely to be populated with roughly the same amount of pixels from the foreground and the background. This brings us back to the first problem, namely, how to define the neighborhood. It is important that the pixels of the neighborhood show consistent disparity values. Inspired by anisotropic post-processing techniques (Banno and Ikeuchi, 2009; Mattoccia, 2009) we define the neighborhood $N(f)$ of a pixel f in correspondence with the spatial proximity and the color similarity to the surrounding pixels

$$N(f) = \{p \mid \Delta_s(f,p) < \theta_s \wedge \Delta_c(f,p) < \theta_c\}\,. \tag{2}$$

The underlying idea is that pixels which belong to a common surface are likely to have a similar appearance.

For the color similarity we use a simple Euclidean distance measure

$$\Delta_c(f,p) = \sum_{a\in\{R,G,B\}} (I_a(f) - I_a(p))^2\,. \tag{3}$$

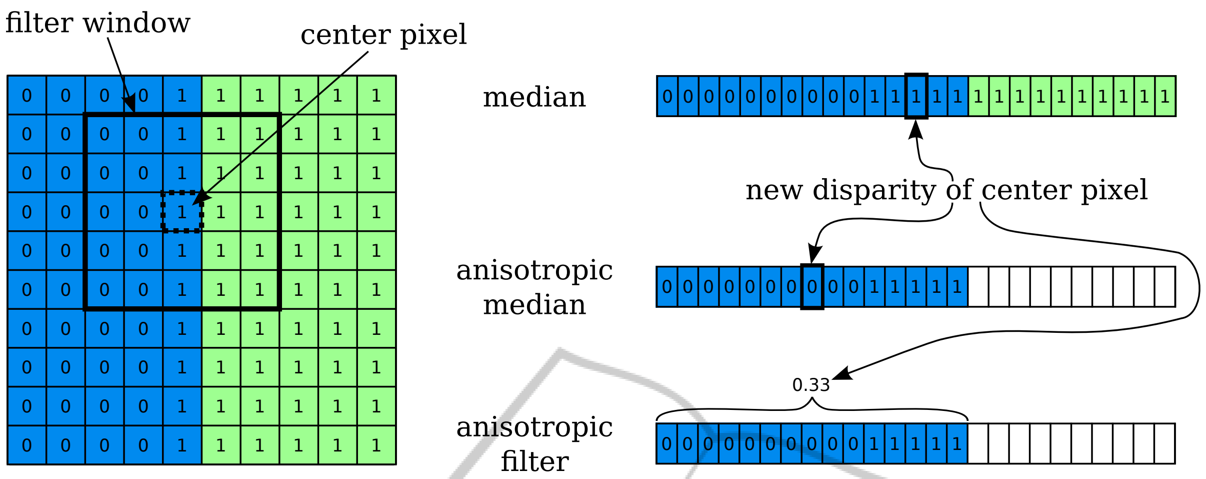

Figure 2: *Anisotropic Median Filter:* On the left side a simplified depth map is displayed. The numbers represent the estimated disparity and the colors indicate the pixel color. Blue pixels are background pixels and green pixels are foreground pixels with a ground truth of disparity of ”0” and ”1”, respectively. As a consequence blue pixels with a disparity of ”1” are wrongly estimated due to the fattening effect. The right side shows the working principle of a median filter, a simple anisotropic (weighted) average filter and the anisotropic median filter for the thick filter window on the left. While the median would replace the dotted center pixel with ”1”, the anisotropic median correctly replaces the center pixel disparity with ”0”. The reason is that it takes only pixels into account that are similar to the center pixel (blue). Although a standard anisotropic averaging filter also considers pixel similarity, it fails of returning the correct value of ”0” because it employs no means of detecting outliers in the disparity values. Thus the filter result of ”0.33” is contaminated by the outlier values ”1” of the blue background pixels.

SCITEPRESS SCIENCE AND TECHNOLOGY PUBLICATIONS

However, for the spatial proximity $\Delta_s(x,p)$ we rather apply the Manhattan distance as this can be realized more efficiently than the Euclidean distance on a pixel grid

$$\Delta_s(f,p) = \sum_{a\in\{x,y\}} |f_a - p_a| \,. \qquad (4)$$

Indeed using the Manhattan distance for spatial proximity corresponds to defining a squared image patch around a center pixel f. Hence, we will skip $\Delta_s(f,p)$ in the following and rather just refer to the size of the filter window from which the neighborhood $N(f)$ is extracted.

Figure 2 displays a simplified example for visualizing the working principle of the anisotropic median filter in comparison to a plain median filter and a simple anisotropic averaging filter. The simple example consists of blue background and green foreground pixels with a ground truth disparity of ”0” and ”1”, respectively. Some of the blue pixels, however, have been assigned a disparity ”1” by the stereo algorithm (fattening effect). By applying a plain median filter the wrong disparities are not removed because they have enough support in the filter window. In contrast, the anisotropic median filter considers only pixels in the filter window that have a color similar to the center pixel (blue dotted pixel in Fig. 2). Thus the wrong disparity ”1” has much less support and the anisotropic median replaces the center pixel’s disparity by ”0”. In comparison to this a standard averaging anisotropic filter will fail as depicted at the bottom of Fig. 2. Since all blue pixels get the same weight the outlier pixels contaminate the filter result. This is a typical problem of anisotropic filters, i.e. disparity outliers are not considered.

4 COMPUTATIONAL CONSIDERATIONS

For maps or images which have only a small integer range the plain median filter can be calculated efficiently and quasi independently of the filter size (Perreault and Hébert, 2007). Unfortunately, this cannot be applied to the anisotropic median filter for disparity refinement. The first reason is, that the quasi size-independent runtime is realized via running histograms. These, however, will get very large for subpixel accurate disparity maps. A second but more severe problem is that due to the anisotropic processing the neighborhood $N(p)$ of a pixel p cannot be computed by taking the neighborhood $N(p-1)$ and updating it for pixel p. Because of this the neighborhood $N(p)$ must be constructed for every pixel (p) independently, which also means that the anisotropic median cannot be calculated in a running filter fashion.

The naïve approach for finding the median of a list of n unsorted elements is to first sort the list and

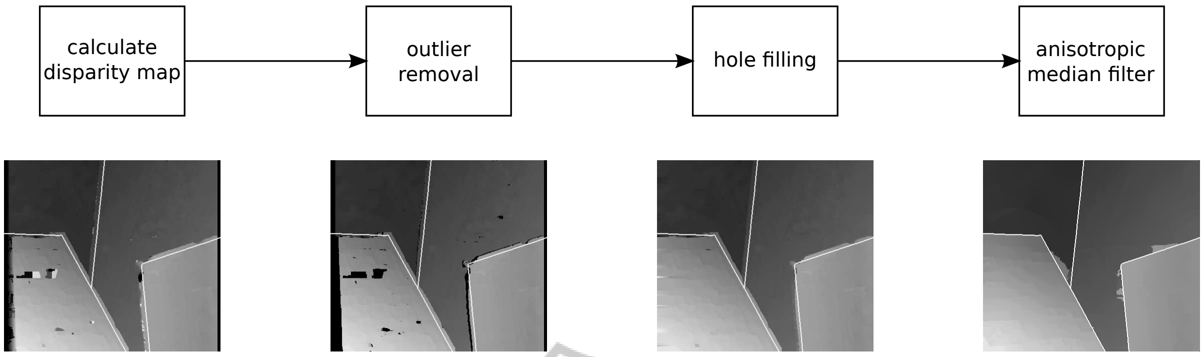

Figure 3: Processing pipeline for anisotropic median filtering. For an optimal result, first, outliers have to be removed. The resulting holes are either filled by means of applying the anisotropic median exclusively to the holes or by linear interpolation. Eventually, the anisotropic median is applied to the full disparity map. The white lines in the disparity maps below the flow chart show the ground truth position of the main depth discontinuities.

then select the median entry. As the best runtime for any sorting algorithm based on the comparison of whole keys is bound by $\Omega(n\log(n))$ the naïve median is bound alike. A better way is to use *quickselect* (Hoare, 1961). Although this has a worst case runtime of $\mathcal{O}(n^2)$ its average runtime is $\mathcal{O}(n)$. Since we apply the anisotropic median on every pixel for refining a disparity map, the high worst case runtime has only very little effect. Altogether, applying the anisotropic median to a whole disparity map has an expected runtime of $\mathcal{O}(\bar{n}m)$ with $\bar{n}$ being the average neighborhood size and m being the number of pixels in the disparity map. This means that as long as $\bar{n}$ is comparable to the disparity search range d, the runtime of the anisotropic median is comparable to the runtime of block-matching stereo which typically has a runtime of $\mathcal{O}(dm)$.

5 PROCESSING PIPELINE

In order to get the best performance of the *anisotropic median* (AM) filter we combine it with means to remove outliers from the disparity map. If not removed, outliers that populate the low-texture regions can hamper the AM filter. The overall pipeline we employ is depicted in Fig. 3. For outlier removal we use a simple technique proposed in (Fua, 1993). The idea is to remove small areas with constant disparity. We extend this a bit by removing only those regions whose disparities differ substantially from the surrounding. It is of course possible to apply also other techniques like a left-right consistency check (Fua, 1993). In general, it is best to apply such techniques before the AM filtering. However, in most cases the removal of the small erroneous areas is sufficient.

As a matter of fact, the outlier removal punches holes into the disparity map. These holes would lead to a positive bias in the evaluation, if AM would be applied directly to the perforated disparity map. The reason is that the hole pixels are marked with invalid (negative) disparity values. Thus any estimation of a real disparity value will be better as the invalid marking values which will of course reduce the overall disparity error. In order to prevent this bias in the evaluation, we apply the AM filter first to the hole pixels only and consider this as a hole filling post-processing step whose resulting disparity map is used as base line. Since the hole filling does not alter the other disparity values, the disparity map after the hole filling still contains the fattening errors (see Fig. 3).

After the hole filling step follows the actual AM filter step. This is applied to the whole disparity map. The difference between the disparity error after the hole filling step and after the AM filter step is used for evaluating our proposed AM filter in the following.

6 EXPERIMENTS

In this section, we assess the proposed *anisotropic median* (AM) filter by using the Middlebury data set (Scharstein and Szeliski, 2002). In the first experiment, the effectiveness of AM as disparity map refinement is evaluated for different block-matching stereo approaches. We apply AM to block-matching with *sum of absolute difference* (SAD) (Scharstein and Szeliski, 2002), *normalized cross-correlation* (NCC) (Scharstein and Szeliski, 2002), *summed normalized cross-correlation* (SNCC) (Einecke and Eggert, 2010) and *rank* and *census* transform (Zabih and Woodfill, 1994).

In the following evaluations, the color stereo images are always transformed to gray level images for block-matching stereo. Furthermore, *rank* and *census* require a certain image patch size for transform-

Table 1: Improvement of block-matching stereo by AM post-processing. The block-matching methods used are: *sum of absolute difference* SAD (Scharstein and Szeliski, 2002), *normalized cross-correlation* NCC (Scharstein and Szeliski, 2002), *summed normalized cross-correlation* SNCC (Einecke and Eggert, 2010) and *rank* and *census* transform (Zabih and Woodfill, 1994). The upper table compares the performance of the different methods after the hole filling step (”+ fill”) and after the AM filter step (”+ AM”) (see also Fig. 3). The performance is measured by means of the percentage of bad pixels (Scharstein and Szeliski, 2002) with a disparity error threshold of 0.5. As the results show, AM leads to an improvement in **all** cases. Moreover, the average gain (average difference between the error of ”+ fill” and ”+ AM”) highlights that the improvement is highest for regions of depth discontinuity. The lower table lists the parameters used for the different block-matching methods.

	Tsukuba			Venus			Teddy			Cones		
Algorithm	nocc	all	disc	nocc	all	disc	nocc	all	disc	nocc	all	disc
SAD + fill	11.1	12.2	21.3	7.62	8.54	22.8	24.5	30.1	42.7	14.2	21.8	29.5
SAD + AM	8.95	9.61	17.9	3.26	3.73	9.99	21.2	27.0	37.4	10.8	18.0	22.9
RT + fill	10.9	11.8	25.0	4.18	5.13	17.4	13.8	20.8	34.3	7.89	16.0	21.7
RT + AM	9.4	9.9	21.9	1.75	2.32	9.91	12.7	19.8	30.3	7.63	15.1	19.3
NCC + fill	9.84	10.9	24.0	5.03	5.97	21.9	15.7	21.9	37.3	9.16	16.7	23.4
NCC + AM	8.44	9.13	19.5	1.75	2.26	10.2	12.8	18.9	31.3	6.45	13.6	17.7
SNCC + fill	10.3	11.2	21.4	3.44	4.28	14.9	12.3	18.5	30.6	6.11	13.7	16.8
SNCC + AM	9.23	9.89	19.2	1.65	2.08	8.56	11.1	17.2	27.3	5.58	12.8	15.1
Census + fill	11.0	11.7	21.1	3.75	4.61	15.8	12.3	18.7	30.7	6.31	14.0	17.4
Census + AM	9.14	9.60	18.9	1.70	2.18	9.08	11.1	17.2	27.4	6.11	13.2	15.9
average gain	**1.60**	**1.75**	**3.08**	**2.78**	**3.19**	**9.01**	**1.94**	**1.98**	**4.38**	**1.42**	**1.90**	**3.58**

Algorithm	SAD	RT	NCC	SNCC	Census
block-matching size	7x7	7x7	5x5	5x5	5x5
AM filter size	21x21	21x21	15x15	17x17	19x19

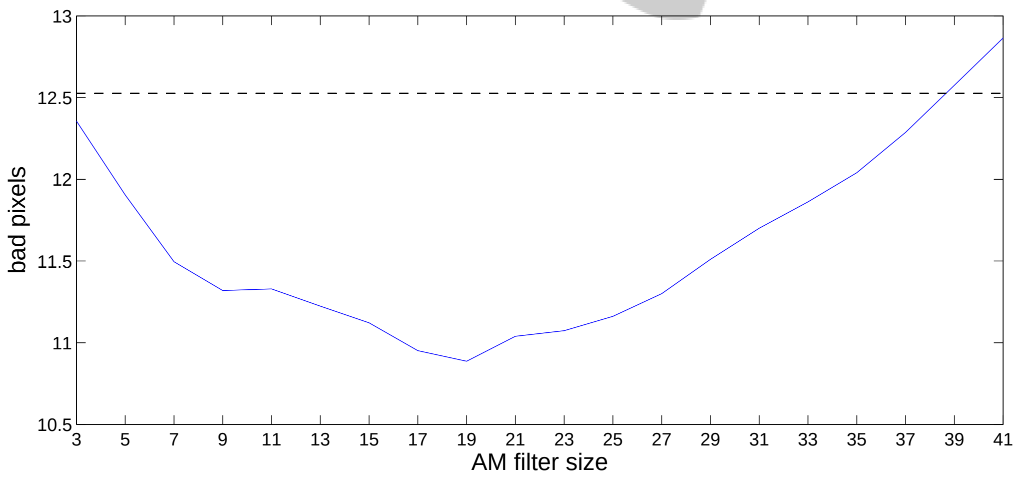

Figure 4: This plot shows the performance (bad pixels percentage combined for all four Middlebury scenes) of AM with respect to its filter size. The dashed line shows the performance of the *census* block-matching after the hole filling step. The blue, solid line shows the performance after applying AM with different filter sizes. There are two things to notice. First, over a large range of filter sizes the additional application of AM improves the results of the plain block-matching result. Second, the best AM filter size of 19x19 pixels is not a strong peak in the error plot. This means that the selection of a good filter size for AM is quite stable which is important for a good generalization.

ing the images. Here we use a patch size of 11x11 for rank transform as proposed in (Einecke and Eggert, 2010) and 7x7 for census transform because this is the largest odd-valued patch-size that can make use of the fast 64-bit (Humenberger et al., 2010) processing. Similarly, we always use a filter size of 3x3 for the first stage of SNCC as proposed in (Einecke and Eggert, 2010). Furthermore, all used block-matching approaches generate sub-pixel accurate disparity maps by fitting quadratic curves into the matching cost.

For the outlier removal step, we apply a left-right consistency check and the removal of homogeneous outlier regions as proposed in (Fua, 1993). The homogeneous outlier regions are detected by means of a simple but fast region grouping algorithm. Please note that the parameters of the outlier removal are fixed for all block-matching approaches and all experiments.

As described in section 5, we first apply the AM filter to the invalid hole pixels and consider this as a hole filling pre-processing in order to prevent a positive bias in the evaluation of the performance of the AM filter. The invalid hole pixels are marked in the disparity map by negative disparity values. Therefore the neighborhood set $N(f)$ for a pixel f needs to be adapted to consider only pixels with valid disparities $d(p) \geq 0$

$$\begin{aligned} N(f) = \{p \mid \quad & \Delta_s(f,p) < \theta_s \ \wedge \\ & \Delta_c(f,p) < \theta_c \ \wedge \\ & d(p) \geq 0\} \,, \end{aligned} \tag{5}$$

in order to ensure the consistency of the disparity list $D(f)$. In some cases this can result in very small neighborhoods $N(f)$ which could lead to wrong results due to an insufficient statistical significance. To prevent this, we demand the neighborhood $N(f)$ to have at least a cardinality of nine. If it has a smaller cardinality, the corresponding pixel f is not processed by the median filtering, so that the pixel's disparity is still invalid. These few remaining hole are filled by a simple linear interpolation.

After the disparity maps have been made dense, the actual AM filter is applied in a single run to the whole disparity map for refinement. The reduction in disparity error by this final filter step is analyzed in the following.

Table 1 shows the performance of five different block-matching approaches right after the hole filling step and after the AM filter step of the processing pipeline discussed in Fig. 3. As the different cost functions have different optimal working parameters we applied a brute-force optimization to find these points in order to render the different results comparable. The optimal parameters are shown at the bottom of Table 1. The measure used in Table 1 is the percentage of bad pixels as proposed in (Scharstein and Szeliski, 2002)

$$b_p = \sum_f |d(f) - GT(f)| > \delta \,, \tag{6}$$

where δ is the disparity error threshold, $d(f)$ is the disparity of pixel f and $GT(f)$ its ground truth disparity. In this evaluation we use a threshold of $\delta = 0.5$ to see how well AM can cope with sub-pixel accurate disparity maps. One might argue that the strong nonlinearity that a median selection involves, destroys the sub-pixel accuracy of a disparity maps. However, the results in Table 1 demonstrate that in all cases AM is able to improve the performance of block-matching stereo. Hence, it is well suited also for sub-pixel accurate maps. It also strikes that in general the improvement for depth discontinuities (disc) is significantly larger than for non-occluding regions (nocc) or the full disparity map (all). This can best be seen in the average gain which is the average (over all tested block-matching approaches) error difference between the filled disparity maps and the AM filtered disparity map (see also Fig. 3). The large improvement in the 'disc' areas confirms the basic idea behind AM of reducing the fattening effect. On the other hand, the improvement for regions without disparity discontinuities reveals that AM surpasses its actual purpose by providing means for a general disparity map improvement.

Figure 4 shows a plot of the disparity error for different AM filter sizes applied to the results of the *census* block-matching. For comparison the *census* performance after the hole filling step is plotted as a dashed line. The plot demonstrates two things. First, over a large range of filter sizes AM improves the results of the plain *census* result. Second, the best AM filter size is not a strong peak in the error plot. This means that the selection of a good filter size for AM is quite stable which is important for a good generalization.

In order to get a better grasp at the actual improvement capabilities of AM, we compare it in a second experiment to the *local consistency* (LC) approach because LC shares similar characteristics with AM and it has already proven itself to be very effective. LC is similar to AM in the following points: First, its processing is constrained to local neighborhoods. Second, it is non-iterative. Third, it is quite fast with a runtime of only a few seconds on a standard PC and, fourth, it has a very small memory footprint.

In this second comparative experiment we use only SNCC block-matching because it showed the best overall performance in Table 1 and can thus be regarded as an upper bound for the other block-matching approaches. For comparison we use the results of SNCC that have been reported in the original paper (Einecke and Eggert, 2010). The authors of that paper applied a similar outlier removal as we do but filled the resulting holes with a depth-discontinuity-aware linear interpolation. In order to be comparable to (Einecke and Eggert, 2010) we also use a non-square filter size of 9x5 for the second stage of the

Table 2: Accuracy evaluation according to (Scharstein and Szeliski, 2002) where an error threshold of 0.5 is used for calculating the bad pixel percentage. The table compares the results of block-matching with SNCC and simple fill-in post-processing as proposed in (Einecke and Eggert, 2010) against post-processing SNCC block-matching with *local consistency* LC (Mattoccia, 2009) (SNCC+LC) and the proposed *anisotropic median* AM filter (SNCC+AM). The average ranks are taken from the online Middlebury benchmark at the time of submission (February 2012) to this online benchmark. For further comparison the then top ranked approach graph-cut + segment border (GC+SB) (Chen et al., 2009) (for $\delta = 0.5$) is also shown. Please note that SNCC and SNCC+AM compute sub-pixel disparity values while SNCC+LC computes integer disparities. This might introduce a negative bias for the results of LC in this table. See Table 3 for a comparison with $\delta = 1.0$

	avg	Tsukuba			Venus			Teddy			Cones		
Algorithm	Rank	nocc	all	disc	nocc	all	disc	nocc	all	disc	nocc	all	disc
SNCC	25.3	11.3	12.3	27.5	2.35	3.23	15.4	10.6	15.2	28.6	4.71	11.1	13.2
SNCC+LC	13.2	10.3	11.2	16.4	2.14	3.15	9.98	9.56	17.3	24.9	4.46	13.4	10.5
SNCC+AM	10.5	9.96	10.4	19.7	0.76	1.11	6.23	8.70	14.3	23.2	4.47	11.1	12.4
GC+SB	8.6	6.87	7.30	15.3	0.20	0.31	2.44	7.59	9.14	17.5	10.5	11.2	14.4

Table 3: Accuracy evaluation like in Table 2 but with an error threshold of 1.0.

	avg	Tsukuba			Venus			Teddy			Cones		
Algorithm	Rank	nocc	all	disc	nocc	all	disc	nocc	all	disc	nocc	all	disc
SNCC	70.6	5.17	6.08	21.7	0.95	1.73	12.0	8.04	11.1	22.9	3.59	9.02	10.7
SNCC+LC	40.5	2.02	2.76	7.76	0.24	1.00	3.39	6.14	14.0	16.3	2.42	10.0	6.32
SNCC+AM	43.4	3.21	3.57	13.6	0.22	0.45	3.01	6.41	10.4	17.7	3.11	8.61	9.27
GC+SB	25.7	1.47	1.82	7.86	0.19	0.31	2.44	4.25	5.55	10.9	4.99	5.78	8.66

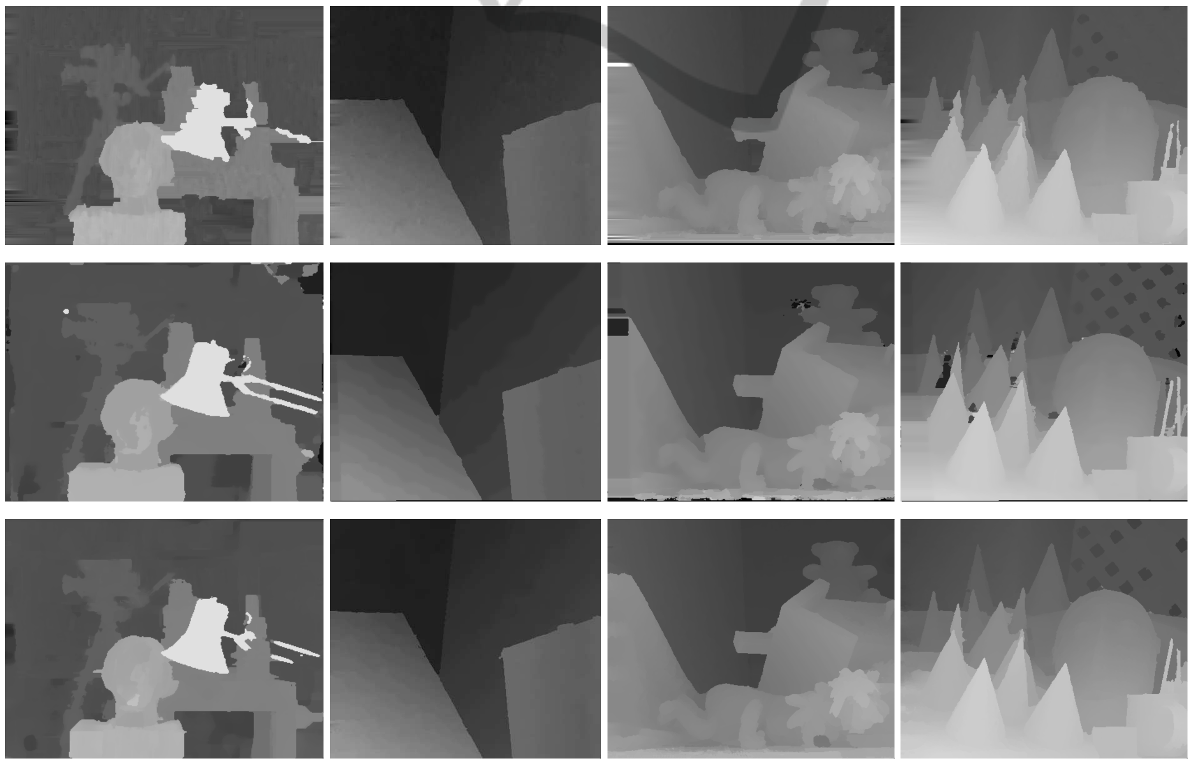
Figure 5: From top to bottom: disparity maps generated by block-matching with SNCC + linear interpolation (Einecke and Eggert, 2010) copied from the Middlebury online database, SNCC + LC and SNCC + AM. Please note that SNCC + linear interpolation and SNCC + AM compute sub-pixel disparity values while SNCC + LC computes integer disparities.

SNCC block-matching. Furthermore, we apply LC as described in (Mattoccia, 2009), i.e. without the processing pipeline described in this paper. Again we optimized the parameters for each approach for comparison. For AM we found a filter size of 19x19 to be most effective and for LC the best parameter set is $R = 39\text{x}39$, $\gamma_s = 31$, $\gamma_c = 21$, $\gamma_t = 13$, $\rho = 40$ (please note that this corresponds to the notation used in (Mattoccia, 2009)).

The results of the comparison of the original SNCC, SNCC plus LC and SNCC plus AM are shown in Table 2 and Fig. 5. Again the bad pixel percentage with an error threshold of 0.5 is used for this assessment. Furthermore, we used the temporary online benchmark feature of the Middlebury website to see how the average rank of the SNCC block-matching would change in the Middlebury comparison when applied with the more advanced post-processing of LC or AM. As can be seen AM and LC improve the average rank of SNCC from 25.3 to 10.5 and 13.2, respectively. In fact SNCC+AM achieves overall the second best result (average rank) behind graph-cut + segment border (GC+SB) (Chen et al., 2009) in the Middlebury online benchmark (February 2012) for $\delta = 0.5$. SNCC+LC would give the third best result.

One reason for the slightly worse results of LC might be that LC is actually not considering sub-pixel accuracies. In order to test this hypothesis Table 3 shows the performance for a disparity error threshold of 1.0. Indeed, the results in Table 3 demonstrate that LC is slightly better than AM for this less strict threshold. Thus, one can conclude that overall LC and AM show a very similar performance but that AM is more advantageous for sub-pixel accurate disparity maps while LC is more accurate for integer-valued disparity maps.

6.1 Runtime

The runtime of AM is about 850ms for the teddy scene on one core of an Intel Core i5 with 3.2GHz. Considering that fast block-matching takes around 150ms (Einecke and Eggert, 2010; Humenberger et al., 2010) for the teddy scene, AM is too slow for a realistic real-time application on a mobile system. In order to improve this, we apply a sparseness technique described for the census transform in (Humenberger et al., 2010). Instead of calculating the median of the whole neighborhood, only pixels in every second row and column are used, i.e. only one fourth of all neighborhood pixels are evaluated. By doing so the runtime decreases to 270ms with a small degradation of the result to an average rank of 12.2 which is still the second best result (February 2012) for $\delta = 0.5$. Hence, the sparse anisotropic median allows for a time efficient post-processing of block-matching approaches.

7 SUMMARY AND DISCUSSION

In this paper, we presented the *anisotropic median* (AM) filter, a novel technique for disparity map post-processing with a focus on the reduction of the fattening effect. The main application we have in mind for this post-processing are block-matching generated disparity maps because these are prone to the fattening effect. The basic idea is to extend the standard median filter by taking only pixels into account that are similar to the center pixel of the filter window. Due to this, disparity values that are inconsistent with similar pixels are replaced by consistent ones. This constitutes an anisotropic smoothness constraint that is applied to the disparity map. Experiments with block-matching stereo and different cost functions demonstrated that in all cases AM leads to a significant improvement of the quality. Furthermore, a comparison with state-of-the-art methods for disparity map refinement shows that AM has a comparable performance but at a much lower computational cost. In fact, we could demonstrate that AM applied to disparity maps of block-matching stereo with summed normalized cross-correlation achieves the second best ranking (February 2012) in the Middlebury stereo benchmark ($\delta = 0.5$) with a total processing time (block-matching plus AM) of 420ms on a single CPU core. This highlights that real-time and accurate stereo is possible with restricted resources as commonly found on mobile robots and platforms.

We identified some issues of AM that need to be tackled in future work. Currently, we use a simple region detection method to remove outlier regions that might negatively influence the performance of the AM filter. Although this worked reliably with a fixed parameter setting in our experiments, it is not guaranteed to work in general. Hence, it would be preferable to replace this with a more concise technique. Second, the used Euclidean distance over RGB values is known to be a weak color similarity measure. For future investigations it is important to test and compare other color spaces. Third, our experiments involved mainly stereo data with colorful scenes. It has to be analyzed in future work how the AM filter is coping with less saturated and monochromatic images. This is especially important for real-world applications where the images typically exhibit only weak color contrasts. Fourth, the speed of AM is not fully satisfying yet. Further strategies have to be introduced before AM is really applicable to real-time mobile robotic systems. One way to reduce the computational cost is to use only one of the RGB color channels or the hue channel of the HSV space or just gray-level images. However, as discussed above this might reduce the accuracy. On the other hand, AM is currently using the pixel color information of one image only. A symmetric approach as proposed in (Mattoccia, 2009) could further improve accuracy, however, at the cost of an increased computational effort. This means one goal of the future work is also to optimize the different processing alternatives for a good trade-off between speed and accuracy.

ACKNOWLEDGEMENTS

The authors would like to thank Stefano Mattoccia from Dipartimento di Elettronica Informatica e Sistemistica (DEIS) of the University of Bologna for applying his *local consistent* stereo method to our SNCC data for comparison.

REFERENCES

Banno, A. and Ikeuchi, K. (2009). Disparity map refinement and 3D surface smoothing via directed anisotropic diffusion. In *3DIM Workshop*, pages 1870 – 1877.

Chen, W., Zhang, M., and Xiong, Z. (2009). Segmentation-based stereo matching with occlusion handling via region border constrains. *CVIU*.

Einecke, N. and Eggert, J. (2010). A two-stage correlation method for stereoscopic depth estimation. In *DICTA*, pages 227–234.

Fua, P. (1993). A parallel stereo algorithm that produces dense depth maps and preserves image features. *Machine Vision and Applications*, 6(1):35–49.

Heo, Y. S., Lee, K. M., and Lee, S. U. (2008). Illumination and camera invariant stereo matching. In *CVPR*, pages 1–8.

Hirschmüller, H. (2005). Accurate and efficient stereo processing by semi-global matching and mutual information. In *CVPR*, pages II: 807–814.

Hoare, C. A. R. (1961). Algorithm 65: Find. *Communication of the ACM*, 4(7):321–322.

Humenberger, M., Zinner, C., Weber, M., Kubinger, W., and Vincze, M. (2010). A fast stereo matching algorithm suitable for embedded real-time systems. *CVIU*, 114(11):1180–1202.

Lucas, B. D. and Kanade, T. (1981). An iterative image registration technique with an application to stereo vision. In *IJCAI*, pages 674–679.

Matthies, L., Kanade, T., and Szeliski, R. (1989). Kalman filter-based algorithms for estimating depth from image sequences. *IJCV*, 3(3):209–238.

Mattoccia, S. (2009). A locally global approach to stereo correspondence. In *3DIM Workshop*, pages 1763–1770.

Mattoccia, S. (2010). Fast locally consistent dense stereo on multicore. In *ECVW*, pages 69–76.

Perona, P. and Malik, J. (1990). Scale-space and edge detection using anisotropic diffusion. *IEEE Trans. Pattern Anal. Mach. Intell.*, 12(7):629–639.

Perreault, S. and Hébert, P. (2007). Median filtering in constant time. *IEEE Transactions on Image Processing*, 16(9):2389–2394.

Scharstein, D. and Szeliski, R. (2002). A taxonomy and evaluation of dense two-frame stereo correspondence algorithms. *IJCV*, 47(1-3):7–42.

Sun, D., Roth, S., and Black, M. J. (2010). Secrets of optical flow estimation and their principles. In *CVPR*, pages 2432–2439.

Sun, X., Mei, X., Jiao, S., Zhou, M., and Wang, H. (2011). Stereo matching with reliable disparity propagation. In *3DIMPVT*, pages 132–139.

Tian, Q. and Huhns, M. N. (1986). Algorithms for subpixel registration. *CVGIP*, 35(2):220–233.

Wang, L., Liao, M., Gong, M., Yang, R., and Nister, D. (2006). High-quality real-time stereo using adaptive cost aggregation and dynamic programming. In *3DPVT*, pages 798–805.

Yang, Q., Yang, R., Davis, J., and Nistér, D. (2007). Spatial-depth super resolution for range images. In *CVPR*, pages 1–8.

Yoon, K.-J. and Kweon, I. S. (2006). Adaptive support-weight approach for correspondence search. *IEEE Trans. Pattern Anal. Mach. Intell.*, 28:650–656.

Zabih, R. and Woodfill, J. (1994). Non-parametric local transforms for computing visual correspondence. In *ECCV*, pages 151–158.

SCITEPRESS SCIENCE AND TECHNOLOGY PUBLICATIONS